Geometrical Properties of the Manganese(IV)/Iron(III) Cofactor of *Chlamydia Trachomatis* Ribonucleotide Reductase Unveiled by Simulations of XAS Spectra

*Eduardo M. Sproviero**

Department of Chemistry and Biochemistry, University of the Sciences in Philadelphia, 600 S. 43rd St., Philadelphia, PA 19104, USA. Fax: +1 215 596 8543; E-mail: e.sproviero@usciences.edu

Table of contents

- **Figure S8.** Scattering paths used in the EXAFS fittings of models **1** to **4**.
- **Figure S9.** Mn and Fe *K*-edge EXAFS spectra simulations of models **1-4**, using parameters computed with Protocol III.
- **Figure S10.** Mn and Fe *K*-edge EXAFS spectra simulations of models **1-4**, using parameters computed with Protocol IV.
- **S2.** Maximum number of variables. The Stern Formula
- **Table S7.** Mn-Fe distances of models **1-4** optimized with different basis sets.
- **Table S8 to S11.** Absorber-scatterer distance changes (Δr) and ΔE_0 from Mn and Fe *K*-edge spectra obtained with Protocol III for models **1** to **4**.
- **Table S12 to S15.** DWFs, absorber-scatterer distance changes (Δr) and ΔE_0 from Mn and Fe *K*-edge spectra obtained with Protocol IV for models **1** to **4**.
- **Table S16.** Mn-Fe lengths obtained with Protocols III and IV applied to models **1** to **4**.
- **S3.** Protocols I to III applied to a test model.
- **S4.** Cartesian coordinates of models 1-4, optimized with the combined 6-31G basis set.

S1. Shells, paths, and Debye-Waller factors in the EXAFS equation

The EXAFS signal is defined as the normalized, oscillatory part of the absorption coefficient $\mu(E)$ with respect to the isolated atomic-background absorption $\mu_0(E)$:

$$\chi(k) = \frac{\mu(k) - \mu_0(k)}{\mu_0(k)} \tag{1}$$

The most basic form of the EXAFS equation could be expressed as a thermal average:[1]

$$\chi(k) = \left\langle S_0^2 \sum_i \left(\frac{3\cos^2(\theta_i)}{kr_i^2} |f_i(k;r)| e^{-2r_i/\lambda(k)} exp\{i[2kr_i + \Phi_i(k,r)]\} \right) \right\rangle \tag{2}$$

where k is the wave number for the photoelectron; r_i is the instantaneous distance to the i^{th} neighbor; < ... > represents an average over all sites in the sample; the exponential term exp[-2r_i /$\lambda(k)$] takes account finite elastic mean free paths of photoelectrons $\lambda(k)$ (between 5 and 10 Å for photoelectron energies from 30 to 1000 eV); S_0^2 is an average amplitude reduction factor (its value, usually 0.8-0.9, is the percent weight of the main excitation channel with respect to all possible excitation channels); f_i and Φi are the scattering amplitude and phase shift of atom i; θ_i is the angle between the electric polarization vector of the X-ray beam $\boldsymbol{\varepsilon}$ and the vector $\mathbf{r}_i$ from the center atom to neighboring atom i. The r-dependence of f and Φ is assumed to be weak.

Assuming small disorder and neglecting curved-wave effects from the r_i dependence of f_i, exp(−2r_i /λ), and 1/r_i^2 we have:[2]

$$\chi(k) = S_0^2 \sum_i \left(\frac{3\cos^2(\theta_i)}{kr_i^2} |f_i(k;r)| e^{-2r_i/\lambda(k)} e^{i\Phi_i(k,r)} \right) \left\langle e^{i2kr_i} \right\rangle \tag{3}$$

The dumping factors $e^{-W_i(k)}$ are amplitude reduction parameters accounting for structural and thermal disorder in a sample. Given a scattering path of total length $2r_i$, it is defined by the thermal and configurational average of the oscillatory part of the XAFS signal:

$$\left\langle e^{i2kr_i} \right\rangle = e^{i2kr_i} e^{-W_i(k)} \tag{4}$$

In the weak-disorder limit (or harmonic approximation), this DW factor is a Gaussian, $W_i(k)$ = $2k^2\ \sigma_i^2$, where $\sigma_i^2 = \langle (r_i - R_i)^2 \rangle$ is the mean-square variation in the effective or half-path length R_i = $\langle r_i \rangle$ appearing in the standard XAFS equation, dubbed Debye-Waller factor (DWF).

Some approaches to XAFS analysis use the concept of “shell” or “sphere”, which are

similar but not identical to the "path". A shell is generally regarded as a group of atoms, at roughly the same distance from the central atom. A path, on the other hand, represents a set of atoms through which the photo-electron can scatter from before returning to the central atom. Thus, averaging over angle and grouping atoms of the same atomic number and similar distances into "shells" we obtain:

$$\chi(k) = S_0^2 \sum_{\substack{i \\ shells}} \left(\frac{N_i}{kR_i^2} |f_i(k;r)| e^{-2k^2\sigma_i^2} e^{-2R_i/\lambda(k)} exp\{i[2kR_i + \Phi_i(k,r)]\} \right) \tag{5}$$

where N_i is the coordination number, R_i the average distance, and σ^2_i the mean square variation in distance to atoms in shell i. These are the leading terms in the "cumulant expansion", if $k\sigma$ is not << 1, higher order terms should be considered.

Multiple scattering (MS) is accounted for by summing over MS paths Γ, each of which may be written in the form[3]

$$\chi_\Gamma(p) = S_0^2 Im\left(\frac{e^{-i(\rho_1 + \rho_2 + \cdots + \rho_N + 2\delta l)}}{\rho_1\rho_2 \ldots \rho_N} e^{-2p^2\sigma_\Gamma^2} \times Tr M_l F^N \cdots F^2 F^l \right) \tag{6}$$

where p is the complex photoelectron momentum, ρ_j are p times the path lengths of the i_{ith} leg of the MS path Γ; the **F** matrices describe the scattering from each atom in the path; and **M** is a termination matrix. Usefully, this expression can be expressed similarly to the single scattering (SS) form:[3]

$$\chi(k) = Im \sum_{\substack{i \\ (paths)}} \left(\frac{N_i S_0^2 F_i^{eff}(k)}{kR_i^2} exp\{i[2kR_i + \Phi_i(k)]\} exp\left(-2\sigma_i^2 k^2\right) exp\left(-\frac{R_i}{\lambda(k)}\right) \right) \tag{7}$$

where N_i is the number of atoms of type i within a path of effective length R_i; the dumping factor $\exp(-2\sigma_i^2 k^2)$ takes into account fluctuations of distances due to a structural or thermal disorder along path i, under the assumption of small displacements and Gaussian distributions of distances, and includes the Debye-Waller factor σ_i^2; $F^{eff}_i(k)$ is a scattering amplitude function characteristic of the i^{th} path; and $\Phi_i(k)$ is a phase function that takes account of the varying potential field along which the photoelectron moves.

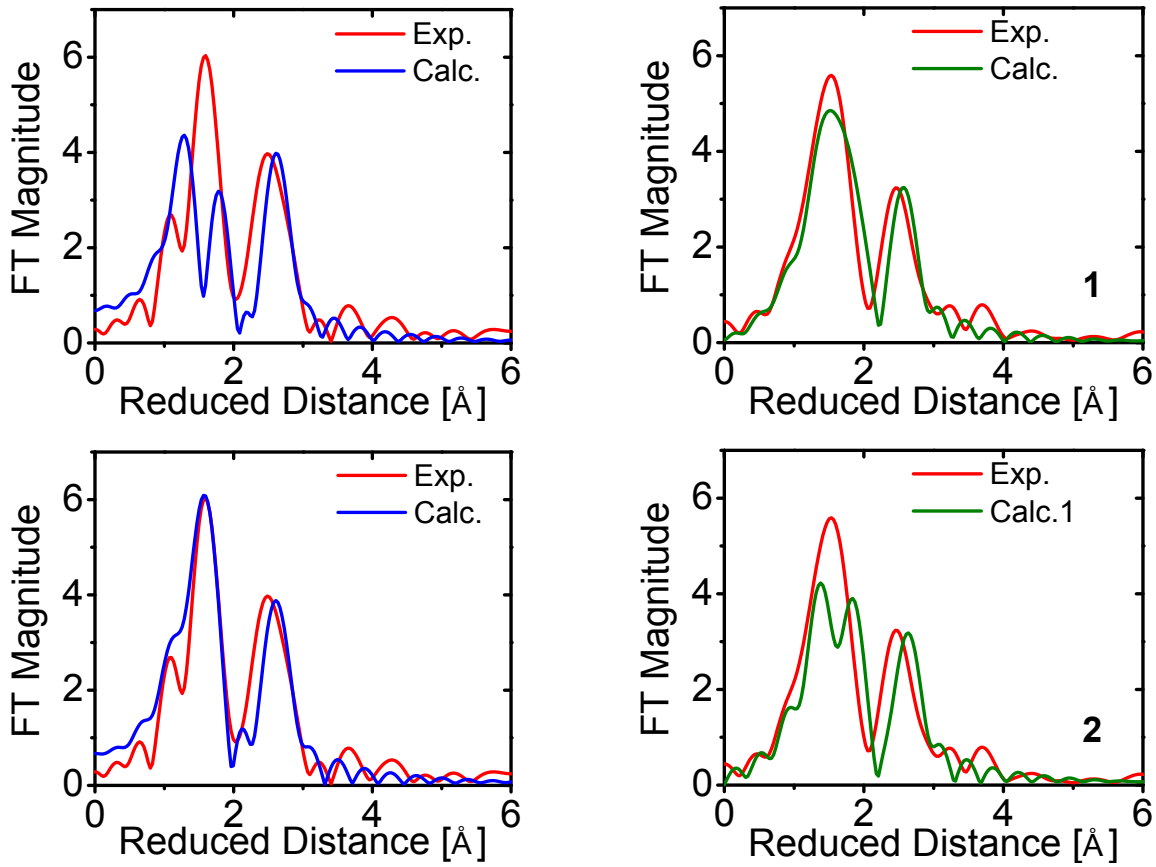

Figure S1. Mn (left) and Fe (right) *K*-edge EXAFS spectra in the *R* space of models **1** and **2** (top to bottom) using geometries obtained by Kwak *et al*., which were computed with spin-unrestricted B3LYP functional with the 6-311+G* basis set on the metals and 6-31G* on the rest of the atoms. The EXAFS spectra (blue for Mn and green for Fe) were computed with DFWs from Younker *et al*. (Protocol I). Red lines are experimental data from Younker *et al.* See Table S1 for details of the fittings.

Table S1. Fittings parameters of Mn and Fe *K*-edge EXAFS in Figure S1, obtained with Protocol I. σ^2 (Å^2) taken from the best fit made in the original experimental study by Younker *et al*.

Model		**Mn**	**Model**		**Fe**
1	σ^2(#1)	**0.0033**	**1**	σ^2(#1-3)	**0.0068**
	σ^2(#2-6)	**0.0038**		σ^2(#4,5)	**0.0027**
	σ^2(#12,15)	**0.0014**		σ^2(#6,9)	**0.0048**
	S_0^2	**0.8**		S_0^2	**1.0**
	ΔE_0	9.52 eV		ΔE_0	9.59 eV
2	σ^2(#1)	**0.0033**	**2**	σ^2(#1-4)	**0.0068**
	σ^2(#2-6)	**0.0038**		σ^2(#5-6)	**0.0027**
	σ^2(#7,16)	**0.0014**		σ^2(#10)	**0.0048**
	S_0^2	**0.8**		S_0^2	**1.0**
	ΔE_0	8.76		ΔE_0	9.59

The numbers in parentheses correspond to the paths included in the calculation of σ^2. The path combination is chosen to be as close as possible to the experimentally-determined shell, and to give the best fit. Bold numbers show the fixed parameters.

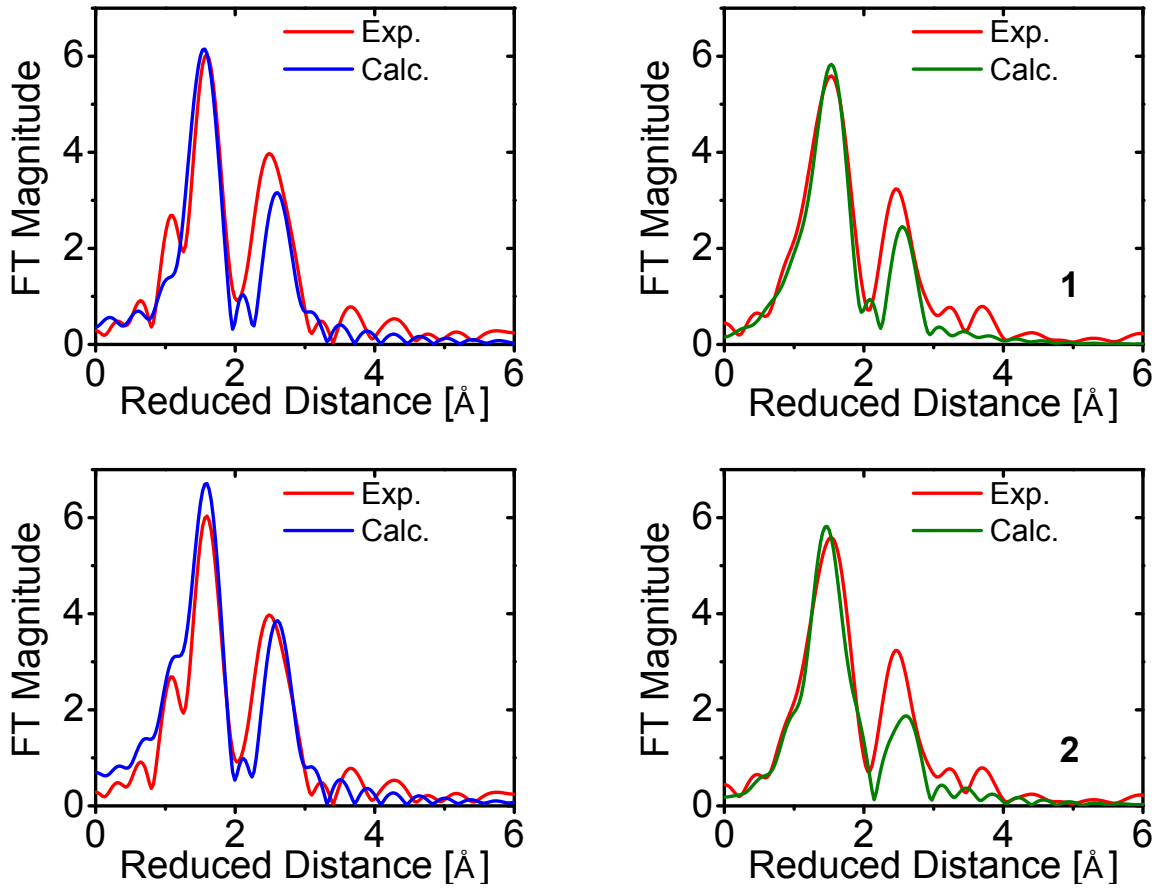

Figure S2. Mn (left) and Fe (right) *K*-edge EXAFS spectra in the *R* space of models **1** and **2** (top to bottom) using geometries obtained by Kwak *et al*., which were computed with spin-unrestricted B3LYP functional with the 6-311+G* basis set on the metals and 6-31G* on the rest of the atoms. The spectra (blue for Mn and green for Fe) were computed with optimized DWFs (Protocol II). Red lines are experimental data from Younker *et al.* See Table S2 for details of the fittings.

Table S2. Fitting parameters of Mn and Fe *K*-edge EXAFS in Figure S2, obtained with Protocol II.

Model		**Mn**	**Model**		**Fe**
1	σ^2(#1,2)	0.0101 Å^2	**1**	σ^2(#1-4)	0.0053 Å^2
	σ^2(#3-6)	0.0010 Å^2		σ^2(#5,6)	0.0100 Å^2
	σ^2(#15)	0.0044 Å^2		σ^2(#9)	0.0068 Å^2
	S_0^2	**0.8**		S_0^2	**1**
	ΔE_0	10.57 eV		ΔE_0	7.77 eV
2	σ^2(#1,2)	0.0100 Å^2	**2**	σ^2(#1-4)	0.0031 Å^2
	σ^2(#3-6)	0.0028 Å^2		σ^2(#5,6)	0.0100 Å^2
	σ^2(#16)	0.0100 Å^2		σ^2(#10)	0.0108 Å^2
	S_0^2	**0.8**		S_0^2	**1.0**
	ΔE_0	7.42 eV		ΔE_0	6.85 eV

The numbers in parentheses correspond to the paths included in the calculation of σ^2. The path combination is chosen to be as close as possible to the experimentally-determined shell, and to give the best fit. Bold numbers show the fixed parameters.

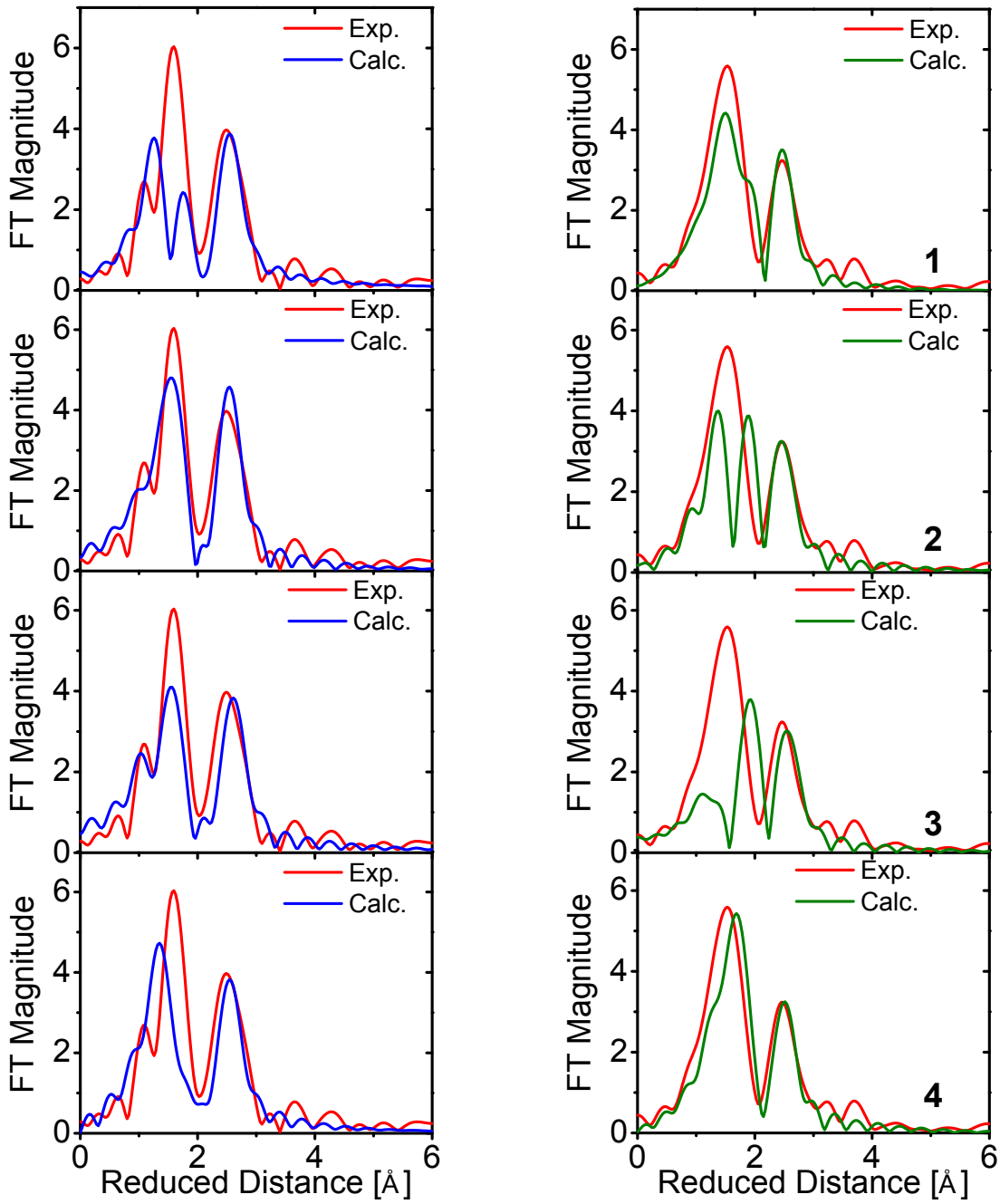

Figure S3. Mn (left) and Fe (right) *K*-edge EXAFS spectra in the *R* space of models **1** to **4** (top to bottom) obtained with the lacvp basis set. The simulated spectra (blue for Mn and green for Fe) were computed with DFWs from Younker *et al.* (Protocol I). Red lines are experimental data from Younker *et al.* See Table S3 for details of the fittings.

Table S3. Fitting parameters of Mn and Fe *K*-edge EXAFS in Figure S3, obtained with Protocol I. σ^2 (Å^2) taken from the best fit made in the original experimental study by Younker *et al*.

Model		**Mn**	**Model**		**Fe**
1	σ^2(#1,2)	**0.0033**	**1**	σ^2(#1)	**0.0068**
	σ^2(#3-8)	**0.0038**		σ^2(#2-6)	**0.0027**
	σ^2(#9-11)	**0.0014**		σ^2(#7-9)	**0.0048**
	S_0^2	**0.8**		S_0^2	**1.0**
	ΔE_0	5.98 eV		ΔE_0	9.34 eV
2	σ^2(#1,2)	**0.0033**	**2**	σ^2(#1-3)	**0.0068**
	σ^2(#2-14)	**0.0038**		σ^2(#4-6)	**0.0027**
	σ^2(#15,16)	**0.0014**		σ^2(#7)	**0.0048**
	S_0^2	**0.8**		S_0^2	**1.0**
	ΔE_0	4.59 eV		ΔE_0	10.88 eV
3	σ^2(#1)	**0.0033**	**3**	σ^2(#1-4)	**0.0068**
	σ^2(#2-8)	**0.0038**		σ^2(#5,6)	**0.0027**
	σ^2(#12)	**0.0014**		σ^2(#12)	**0.0048**
	S_0^2	**0.8**		S_0^2	**1.0**
	ΔE_0	10.12 eV		ΔE_0	13.89 eV
4	σ^2(#1,2)	**0.0033**	**4**	σ^2(#1-3)	**0.0068**
	σ^2(#3-6)	**0.0038**		σ^2(#4-6)	**0.0027**
	σ^2(#11)	**0.0014**		σ^2(#12)	**0.0048**
	S_0^2	**0.8**		S_0^2	**1.0**
	ΔE_0	3.88 eV		ΔE_0	12.08 eV

The numbers in parentheses correspond to the paths included in the calculation of σ^2. The path combination is chosen to be as close as possible to the experimentally-determined shell, and to give the best fit. Bold numbers show the fixed parameters.

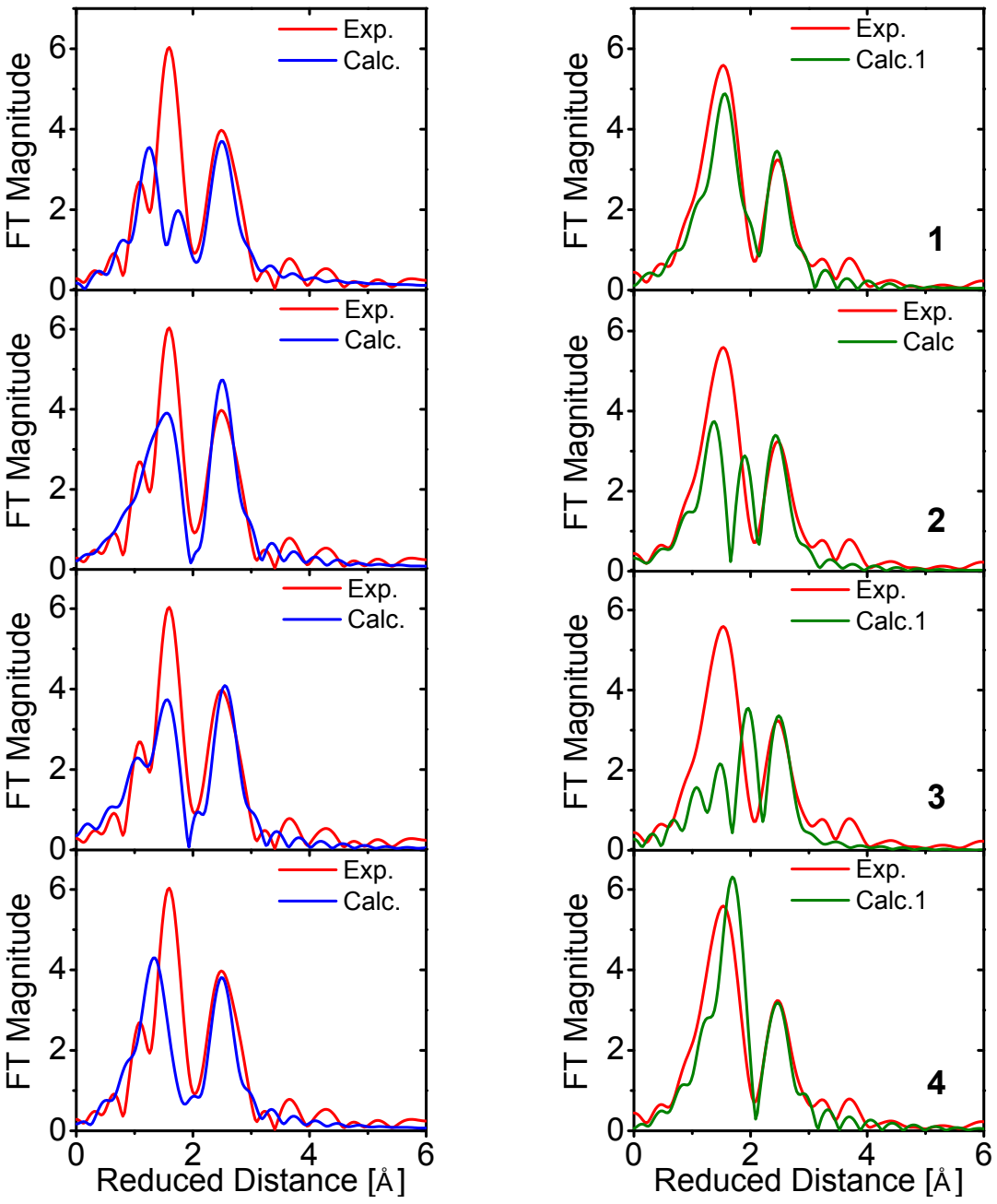

Figure S4. Mn (left) and Fe (right) *K*-edge EXAFS spectra in the *R* space of models **1** to **4** (top to bottom) obtained with the basis set defined as the combination of 6-31G(2df) on the oxo oxygens, and lacvp on the rest of the atoms. Spectra (blue for Mn and green for Fe) were computed with DFWs from Younker *et al.* (Protocol I). Red lines are experimental data from Younker *et al.* See Table S4 for details of the fittings.

Table S4. Fitting parameters of Mn and Fe *K*-edge EXAFS in Figure S4, obtained with Protocol I. σ^2 (Å^2) taken from the best fit made in the original experimental study by Younker *et al*.

Model		**Mn**	**Model**		**Fe**
1	σ^2(#1,2)	**0.0033**	**1**	σ^2(#1)	**0.0068**
	σ^2(#3-8)	**0.0038**		σ^2(#2-6)	**0.0027**
	σ^2(#9-11)	**0.0014**		σ^2(#7-9)	**0.0048**
	S_0^2	**0.8**		S_0^2	**1.0**
	ΔE_0	2.54 eV		ΔE_0	8.36 eV
2	σ^2(#1,2)	**0.0033**	**2**	σ^2(#1-5)	**0.0068**
	σ^2(#3-14)	**0.0038**		σ^2(#6)	**0.0027**
	σ^2(#15,16)	**0.0014**		σ^2(#7-9)	**0.0048**
	S_0^2	**0.8**		S_0^2	**1.0**
	ΔE_0	4.60 eV		ΔE_0	6.80 eV
3	σ^2(#1)	**0.0033**	**3**	σ^2(#1)	**0.0068**
	σ^2(#2-9)	**0.0038**		σ^2(#2-6)	**0.0027**
	σ^2(#10)	**0.0014**		σ^2(#12)	**0.0048**
	S_0^2	**0.8**		S_0^2	**1.0**
	ΔE_0	7.86 eV		ΔE_0	9.59 eV
4	σ^2(#1,2)	**0.0033**	**4**	σ^2(#1-4)	**0.0068**
	σ^2(#3-6)	**0.0038**		σ^2(#5,6)	**0.0027**
	σ^2(#9)	**0.0014**		σ^2(#12)	**0.0048**
	S_0^2	**0.8**		S_0^2	**1.0**
	ΔE_0	9.52 eV		ΔE_0	11.63 eV

The numbers in parentheses correspond to the paths included in the calculation of σ^2. The path combination is chosen to be as close as possible to the experimentally-determined shell, and to give the best fit. Bold numbers show the fixed parameters.

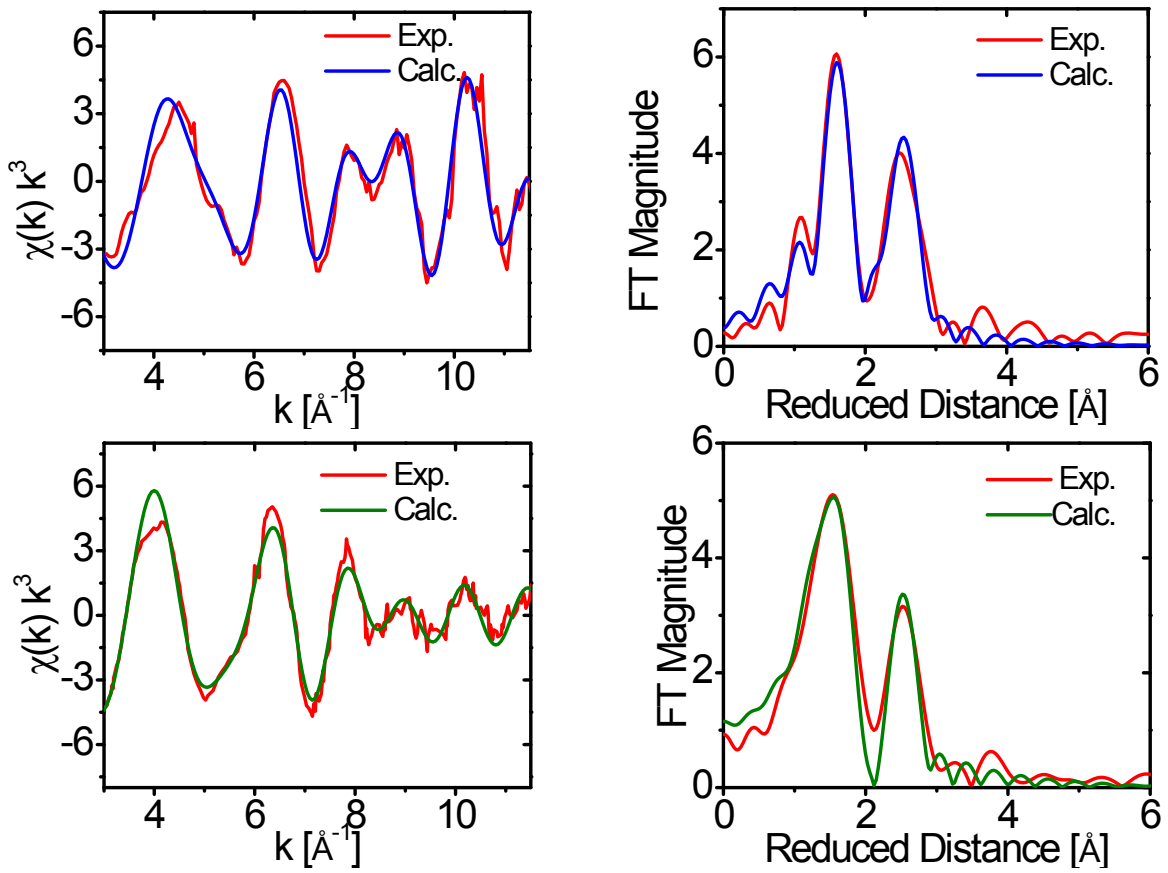

Figure S5. Comparison of Mn (top) and Fe (bottom) *K*-edge fittings of SS paths based on diatomic models (green) with experimental fittings based on shells (red). Absorber-scatterer distances are allowed to vary in the fitting. See Tables 2 and 3 for details of the fittings.

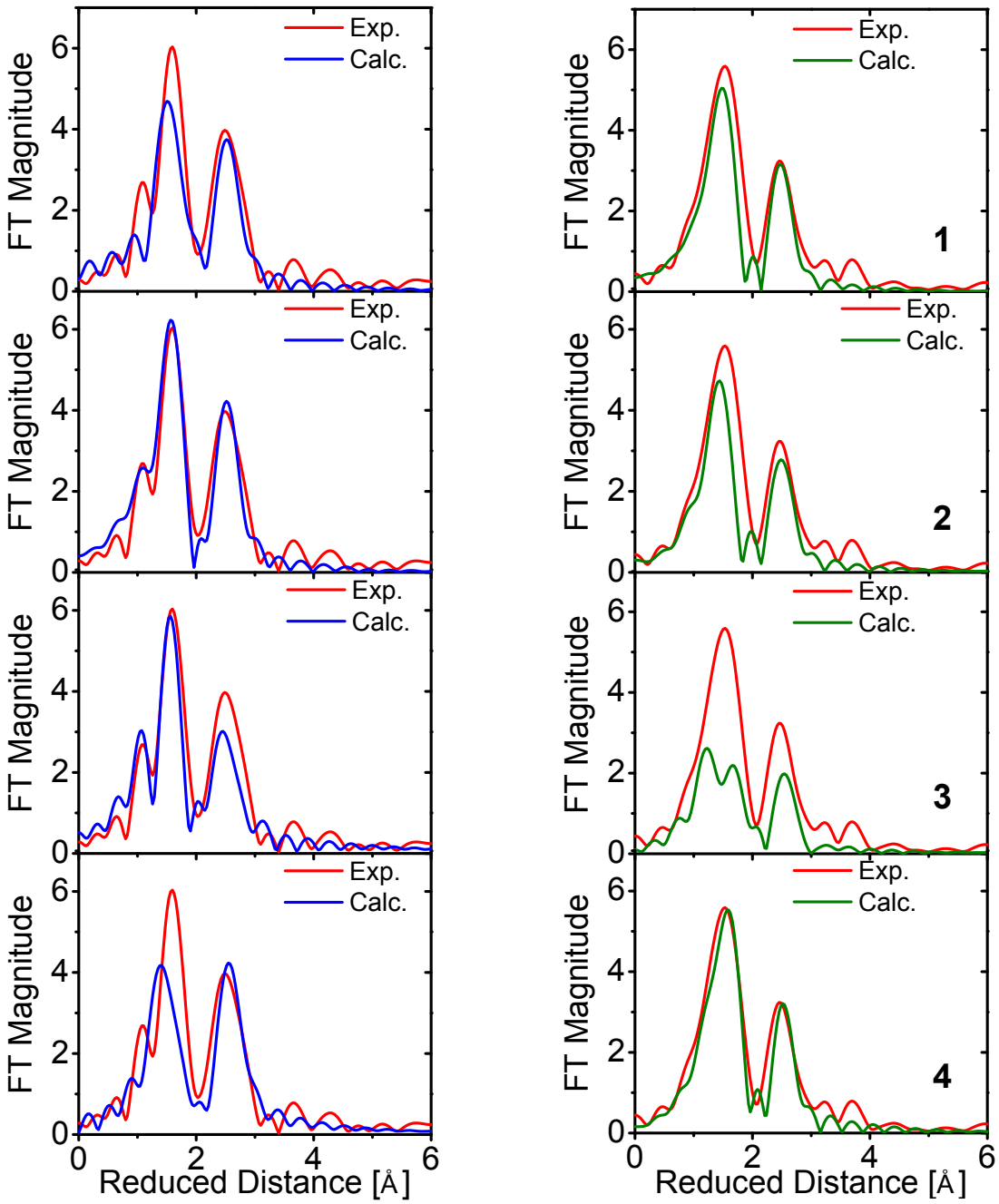

Figure S6. Mn (left, in blue) and Fe (right, in green) *K*-edge EXAFS spectra simulations in the *R* space of models **1** to **4** (top to bottom) obtained with the lacvp basis set. The spectral parameters are computed with the Protocol II. Red lines are experimental data from Younker *et al.* See Table S5 for details of the fittings.

Table S5. S_0^2 and ΔE_0 (eV) parameters of Mn and Fe *K*-edge EXAFS in Figure S6, obtained with Protocol II.

Model		**Mn**	**Model**		**Fe**
1	σ^2(#1,2)	0.0114 Å^2	**1**	σ^2(#1-3)	0.0033 Å^2
	σ^2(#3-5)	0.0010 Å^2		σ^2(#4-6)	0.0010 Å^2
	σ^2(#6,11)	0.0040 Å^2		σ^2(#9)	0.0047 Å^2
	S_0^2	**1.0**		S_0^2	**1.0**
	ΔE_0	7.94 eV		ΔE_0	6.40 eV
2	σ^2(#1)	0.0010 Å^2	**2**	σ^2(#1-3)	0.0055 Å^2
	σ^2(#2-6)	0.0010 Å^2		σ^2(#4-6)	0.0100 Å^2
	σ^2(#9)	0.0011 Å^2		σ^2(#7)	0.0047 Å^2
	S_0^2	**0.7**		S_0^2	**1.0**
	ΔE_0	7.93 eV		ΔE_0	8.80 eV
3	σ^2(#1)	0.0010 Å^2	**3**	σ^2(#1-4)	0.0010 Å^2
	σ^2(#2-6)	0.0010 Å^2		σ^2(#5-6)	0.0101 Å^2
	σ^2(#13)	0.0066 Å^2		σ^2(#12)	0.0065 Å^2
	S_0^2	**0.8**		S_0^2	**1.0**
	ΔE_0	8.41 eV		ΔE_0	10.39 eV
4	σ^2(#1,2)	0.0106 Å^2	**4**	σ^2(#1-4)	0.0044 Å^2
	σ^2(#3-6)	0.0016 Å^2		σ^2(#5-6)	0.0100 Å^2
	σ^2(#11)	0.0021 Å^2		σ^2(#12)	0.0049 Å^2
	S_0^2	**0.7**		S_0^2	**1.0**
	ΔE_0	6.90 eV		ΔE_0	10.19 eV

The numbers in parentheses correspond to the paths included in the calculation of σ^2. The path combination is chosen to be as close as possible to the experimentally-determined shell, and to give the best fit. Bold numbers show the fixed parameters.

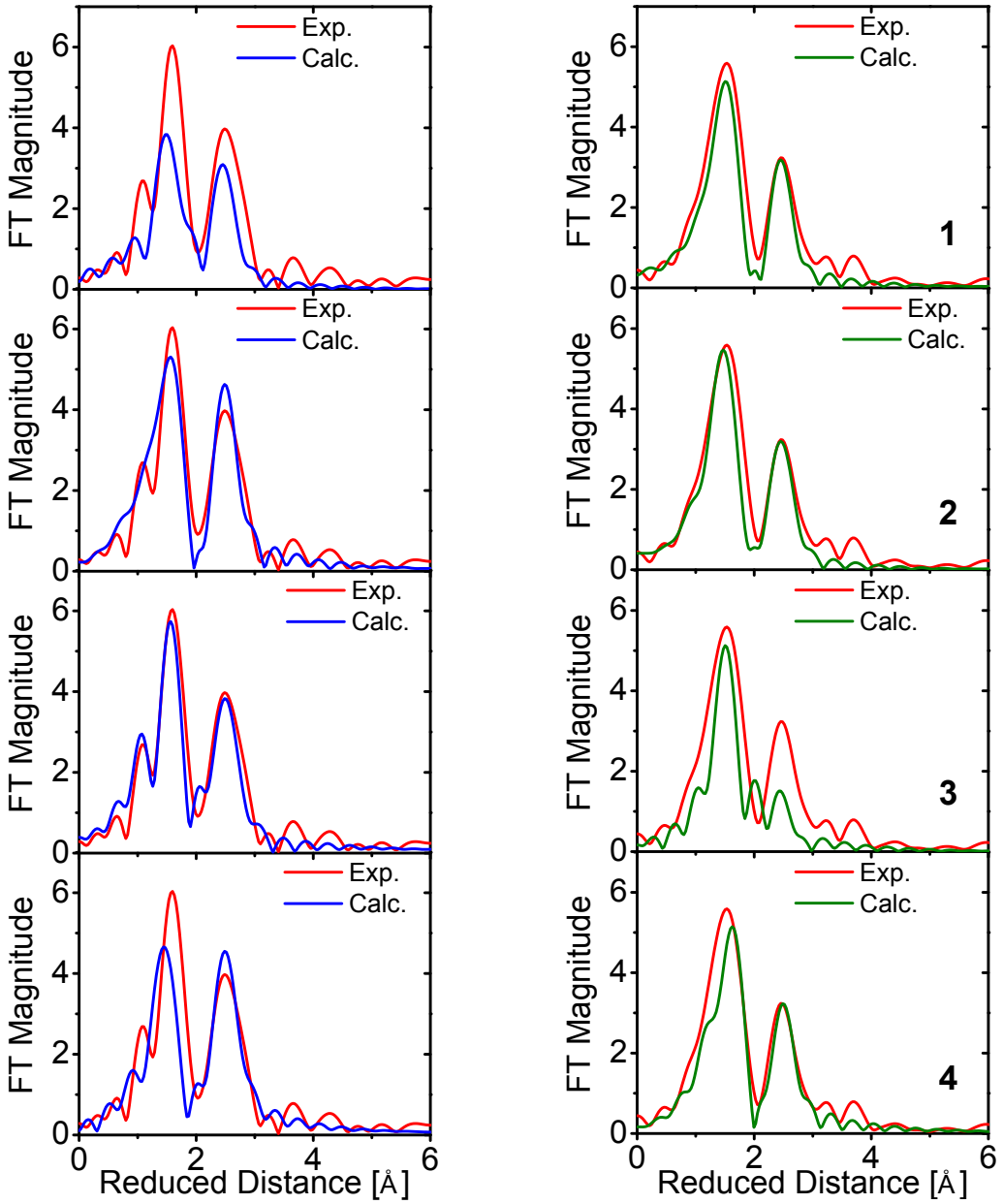

Figure S7. Mn (left, in blue) and Fe (right, in green) *K*-edge EXAFS spectra simulations in the *R* space of models **1** to **4** (top to bottom) obtained with the basis set defined as the combination of 6-31G(2df) on the oxo oxygens, and lacvp on the rest of the atoms. The spectral parameters are computed with the Protocol II. Red lines are experimental data from Younker *et al.* See Table S6 for details of the fittings.

Table S6. Fitting parameters of Mn and Fe *K*-edge EXAFS in Figure S7, obtained with Protocol II.

Model		**Mn**	**Model**		**Fe**
1	σ^2(#1,2)	0.0101 Å^2	**1**	σ^2(#1-3)	0.0020 Å^2
	σ^2(#3-5)	0.0010 Å^2		σ^2(#4-6)	0.0100 Å^2
	σ^2(#6,11)	0.0052 Å^2		σ^2(#9)	0.0053 Å^2
	S_0^2	**1.0**		S_0^2	**1.0**
	ΔE_0	4.42 eV		ΔE_0	5.19 eV
2	σ^2(#1)	0.0010 Å^2	**2**	σ^2(#1-4)	0.0051 Å^2
	σ^2(#2-6)	0.0010 Å^2		σ^2(#5-6)	0.0101 Å^2
	σ^2(#15)	0.0010 Å^2		σ^2(#9)	0.0046 Å^2
	S_0^2	**0.8**		S_0^2	**1.0**
	ΔE_0	5.86 eV		ΔE_0	5.28 eV
3	σ^2(#1)	0.0010 Å^2	**3**	σ^2(#1)	0.0100 Å^2
	σ^2(#2-6)	0.0010 Å^2		σ^2(#2-4)	0.0010 Å^2
	σ^2(#10)	0.0017 Å^2		σ^2(#5,6,12)	0.0100 Å^2
	S_0^2	**0.8**		S_0^2	**1.0**
	ΔE_0	7.50 eV		ΔE_0	9.20 eV
4	σ^2(#1,2)	0.0100 Å^2	**4**	σ^2(#1-4)	0.0048 Å^2
	σ^2(#3-6)	0.0010 Å^2		σ^2(#5-6)	0.0100 Å^2
	σ^2(#9)	0.0010 Å^2		σ^2(#12)	0.0048 Å^2
	S_0^2	**0.8**		S_0^2	**1.0**
	ΔE_0	2.89 eV		ΔE_0	10.03 eV

The numbers in parentheses correspond to the paths included in the calculation of σ^2. The path combination is chosen to be as close as possible to the experimentally-determined shell, and to give the best fit. Bold numbers show the fixed parameters.

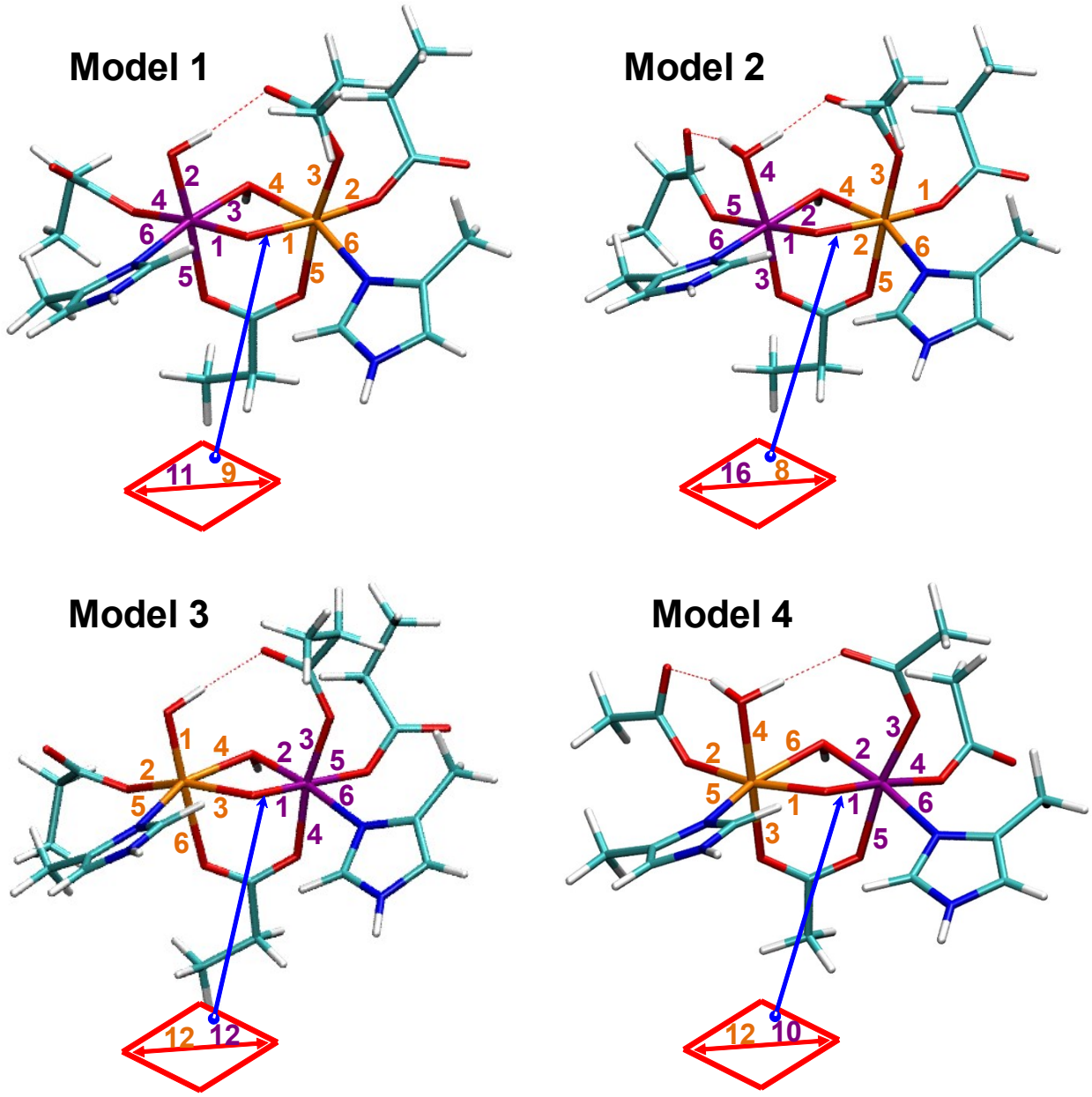

Figure S8. Most relevant scattering paths used in the EXAFS fittings (Mn in purple, and Fe in orange) of models **1** to **4** optimized with the combined 6-31G basis set.

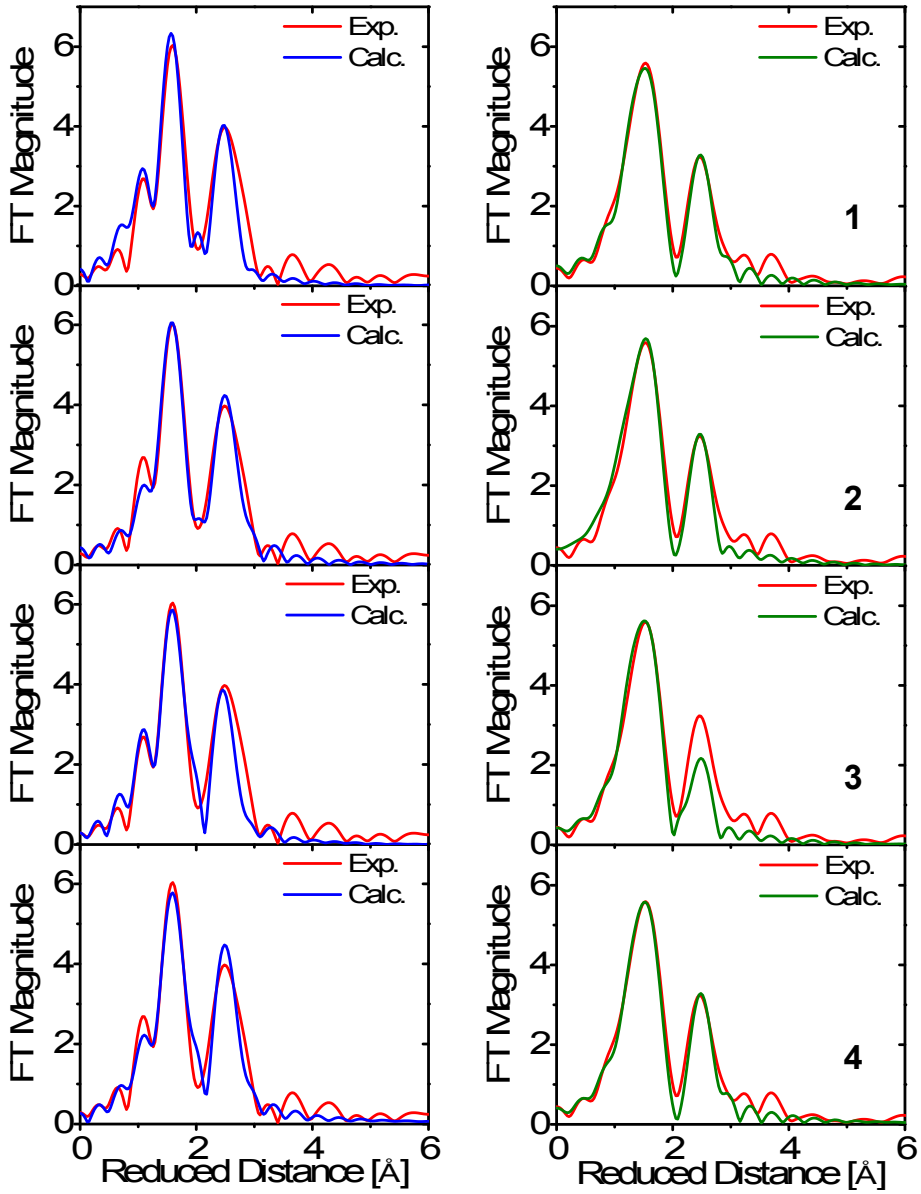

Figure S9. Mn (left panel, blue lines) and Fe (right panel, green lines) *K*-edge EXAFS spectra simulations of model **1**-**4**, using parameters computed with Protocol III. Experimental spectra of Younker *et al.* are shown with red lines. See Tables S8 to S11 for details of the fittings.

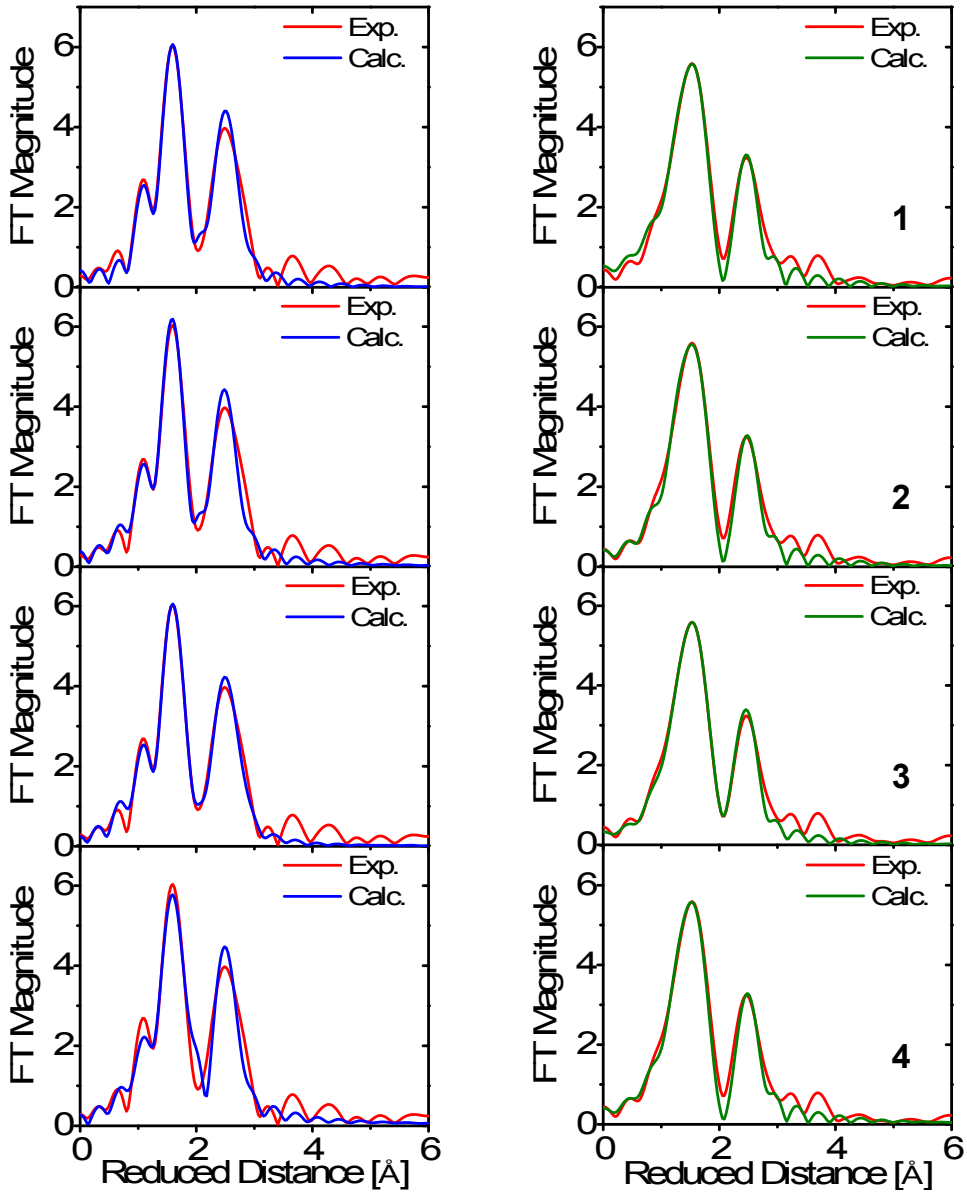

Figure S10. Mn (left panel, blue lines) and Fe (right panel, green lines) *K*-edge EXAFS spectra simulations of models **1**-**4**, using parameters computed with Protocol IV. Experimental spectra of Younker *et al.* are shown with red lines. See Tables S12 to S15 for details of the fittings.

S2. Maximum number of variables. The Stern Formula

Fitting over a range from R_{min} to R_{max}, the number of independent variables N_{ind} that can be obtained from the fitting is given by [Stern, E. A.; Sayers, D. E.; Lytle, F. W. *Phys. Rev. B* 1975, 11 (12), 4836-4846]

$$N_{ind} = \frac{2(k_{max} - k_{min})(R_{max} - R_{min})}{\pi} + 2$$

In our case, Δk = 8.6 Å^{-1}, and R gives meaningful information in the range 1-3 Å. The maximum number of variables obtainable from these ranges is hence up to 13, which is fulfilled in all analyzed cases.

Table S7. Mn-Fe distances of models **1-4** optimized with different basis sets.

Basis Set	Model structure	Mn-Fe distance [Å]
Combined 6-31G	**1**	2.93
	2	2.95
	3	2.99
	4	2.94
Lacvp	**1**	2.93
	2	2.95
	3	2.99
	4	2.94
6-31G(2df) on μ-oxo bridge centers and lacvp on the rest of the molecule	**1**	2.89
	2	2.92
	3	2.96
	4	2.91
Lanl2dz	**1**	3.00
	2	3.01
	3	3.06
	4	3.03

Table S8. Absorber-scatterer distance changes, Δr [Å], and ΔE_0 [kcal/mol] corresponding to Mn and Fe *K*-edge spectra of model **1** in Figure S9, obtained with Protocol III. See Figure S8 for the description of paths.

Mn		**Fe**	
Variable (path#)	**Fitted Value**	**Variable (path#)**	**Fitted Value**
Δr(#1)	-0.01	Δr(#1)	-0.02
Δr(#2)	-0.01	Δr(#2)	-0.02
Δr (#3)	-0.03	Δr(#3)	0.015
Δr (#4)	0.00	Δr(#4)	-0.02
Δr (#5)	-0.06	Δr(#5)	-0.10
Δr (#6)	0.11	Δr(#6)	0.18
Δr (#11)[(a)]	-0.02	Δr(#9) [(a)]	-0.02
ΔE_0	1.49	ΔE_0	3.93
S_0	**1.0**	S_0	**0.9**

[(a)] Mn-Fe intermetal distance. Bold numbers show the fixed parameters.

Table S9. Absorber-scatterer distance changes, Δr [Å], and ΔE_0 [kcal/mol] corresponding to Mn and Fe *K*-edge spectra of model **2** in Figure S9, obtained with Protocol III. See Figure S8 for the description of paths.

Mn		**Fe**	
Variable (path#)	**Fitted Value**	**Variable (path#)**	**Fitted Value**
Δr(#1)	0.01	Δr(#1)	0.05
Δr(#2)	-0.06	Δr(#2)	0.04
Δr (#3)	0.04	Δr(#3)	0.06
Δr (#4)	0.01	Δr(#4)	-0.13
Δr (#5)	0.03	Δr(#5)	-0.16
Δr (#6)	0.17	Δr(#6)	-0.23
Δr (#10)[(a)]	-0.03	Δr(#12)[(a)]	-0.03
Δr (#11)	0.02	Δr(#13)	0.00
Δr (#12)	0.10	Δr(#15)	-0.05
ΔE_0	2.66	ΔE_0	5.42
S_0	**0.9**	S_0	**0.9**

[(a)] Mn-Fe intermetal distance. Bold numbers show the fixed parameters.

Table S10. Absorber-scatterer distance changes, Δr [Å], and ΔE_0 [kcal/mol] corresponding to Mn and Fe *K*-edge spectra of model **3** in Figure S9, obtained with Protocol III. See Figure S8 for the description of paths.

Mn		**Fe**	
Variable (path#)	**Fitted Value**	**Variable (path#)**	**Fitted Value**
Δr(#1)	0.01	Δr(#1)	0.02
Δr(#2)	0.02	Δr(#2)	-0.02
Δr (#3)	0.02	Δr(#3)	0.05
Δr (#4)	0.07	Δr(#4)	-0.09
Δr (#5)	-0.07	Δr(#5)	-0.18
Δr (#6)	0.15	Δr(#6)	-0.23
Δr (#9)	0.00	Δr(#12) [(a)]	-0.08
Δr (#10)	-0.02	–	–
Δr (#11)	-0.02	–	–
Δr (#12) [(a)]	-0.08	–	–
ΔE_0	2.83	ΔE_0	2.07
S_0	**0.8**	S_0	**1.0**

[(a)] Mn-Fe intermetal distance. Bold numbers show the fixed parameters.

Table S11. Absorber-scatterer distance changes, Δr [Å], and ΔE_0 [kcal/mol] corresponding to Mn and Fe *K*-edge spectra of model **4** in Figure S9, obtained with Protocol III. See Figure S8 for the description of paths.

Mn		**Fe**	
Variable (path#)	**Fitted Value**	**Variable (path#)**	**Fitted Value**
Δr(#1)	0.01	Δr(#1)	0.05
Δr(#2)	-0.06	Δr(#2)	0.04
Δr (#3)	0.04	Δr(#3)	0.06
Δr (#4)	0.01	Δr(#4)	-0.13
Δr (#5)	0.03	Δr(#5)	-0.16
Δr (#6)	0.17	Δr(#6)	-0.23
Δr (#10) [(a)]	-0.03	Δr(#12) [(a)]	-0.03
Δr (#11)	0.02	Δr(#13)	0.00
Δr (#12)	0.10	Δr(#15)	-0.05
ΔE_0	2.66	ΔE_0	5.42
S_0	**0.9**	S_0	**0.9**

[(a)] Mn-Fe intermetal distance. Bold numbers show the fixed parameters.

Table S12. DWFs [Å^2], absorber-scatterer distance changes, Δr [Å], and ΔE_0 [kcal/mol] corresponding to Mn and Fe *K*-edge spectra of model **1** in Figure S10, obtained with Protocol IV. See Figure S8 for the description of paths.

Mn		**Fe**	
Variable (path#)	**Fitted Value**	**Variable (path#)**	**Fitted Value**
σ^2 (#1-6)	0.0033	σ^2 (#1-6)	0.0017
σ^2 (#11)	0.0010	σ^2 (#9)	0.0043
Δr(#1)	-0.08	Δr(#1)	0.06
Δr(#2)	0.03	Δr(#2)	-0.16
Δr (#3)	0.03	Δr(#3)	0.09
Δr (#4)	-0.02	Δr(#4)	-0.17
Δr (#5)	-0.15	Δr(#5)	-0.17
Δr (#6)	-0.13	Δr(#6)	-0.15
Δr (#11) [(a)]	-0.02	Δr(#9) [(a)]	-0.02
ΔE_0	1.46	ΔE_0	2.16
S_0	**0.8**	S_0	**1.0**

[(a)] Mn-Fe intermetal distance. Bold numbers show the fixed parameters.

Table S13. DWFs [Å^2], absorber-scatterer distance changes, Δr [Å], and ΔE_0 [kcal/mol] corresponding to Mn and Fe *K*-edge spectra of model **2** in Figure S10, obtained with Protocol IV. See Figure S8 for the description of paths.

Mn		**Fe**	
Variable (path#)	**Fitted Value**	**Variable (path#)**	**Fitted Value**
σ^2 (#1-6)	0.0029	σ^2 (#1-3, 5,6)	0.0010
σ^2 (#16)	0.0016	σ^2 (#7,8)	0.0039
Δr(#1)	-0.01	Δr(#1)	-0.05
Δr(#2)	-0.08	Δr(#2)	0.03
Δr (#3)	-0.06	Δr(#3)	0.00
Δr (#4)	0.00	Δr(#5)	-0.08
Δr (#5)	-0.07	Δr(#6)	-0.07
Δr (#6)	-0.09	Δr(#7)	0.19
Δr (#16) [(a)]	-0.04	Δr(#8) [(a)]	-0.04
ΔE_0	2.809	ΔE_0	7.27
S_0	**0.9**	S_0	**1.0**

[(a)] Mn-Fe intermetal distance. Bold numbers show the fixed parameters.

Table S14. DWFs [Å^2], absorber-scatterer distance changes, Δr [Å], and ΔE_0 [kcal/mol] corresponding to Mn and Fe *K*-edge spectra of model **3** in Figure S10, obtained with Protocol IV. See Figure S8 for the description of paths.

Mn		**Fe**	
Variable (path#)	**Fitted Value**	**Variable (path#)**	**Fitted Value**
σ^2 (#1-2)	0.0022	σ^2 (#1-6)	0.0043
σ^2 (#3-6)	0.0049	σ^2 (#12)	0.0044
σ^2 (#12)	0.0010	–	–
Δr(#1)	-0.00	Δr(#1)	0.02
Δr(#2)	0.03	Δr(#2)	0.06
Δr (#3)	0.03	Δr(#3)	0.05
Δr (#4)	-0.03	Δr(#4)	-0.23
Δr (#5)	-0.05	Δr(#5)	-0.13
Δr (#6)	0.18	Δr(#6)	-0.30
Δr (#12) [(a)]	-0.08	Δr(#12) [(a)]	-0.08
ΔE_0	1.50	ΔE_0	1.29
S_0	**0.8**	S_0	**1.0**

[(a)] Mn-Fe intermetal distance. Bold numbers show the fixed parameters.

Table S15. DWFs [Å^2], absorber-scatterer distance changes, Δr [Å], and ΔE_0 [kcal/mol] corresponding to Mn and Fe *K*-edge spectra of model **4** in Figure S10, obtained with Protocol IV. See Figure S8 for the description of paths.

Mn		**Fe**	
Variable (path#)	**Fitted Value**	**Variable (path#)**	**Fitted Value**
σ^2 (#1-2)	0.0100	σ^2 (#1-3)	0.0010
σ^2 (#3-6)	0.0010	σ^2 (#4-5)	0.0101
σ^2 (#12)	0.0021	σ^2 (#6-12)	0.0042
Δr(#1)	0.00	Δr(#1)	0.04
Δr(#2)	-0.01	Δr(#2)	0.03
Δr (#3)	0.04	Δr(#3)	0.04
Δr (#4)	0.36	Δr(#4)	-0.16
Δr (#5)	0.04	Δr(#5)	0.00
Δr (#6)	-0.17	Δr(#6)	-0.24
Δr (#10) [(a)]	-0.03	Δr(#12) [(a)]	-0.03
ΔE_0	2.16	ΔE_0	5.16
S_0	**0.9**	S_0	**1.0**

[(a)] Mn-Fe intermetal distance. Bold numbers show the fixed parameters.

Table S16. Mn-Fe lengths obtained with Protocols III and IV applied to models **1** to **4**, from Mn and Fe *K*-edge EXAFS. All distances in Å.

Model	**DFT length**	**Δr**		**Suggested length**	
		P III	**P IV**	**P III**	**P IV**
1	2.93	-0.02	-0.02	2.91	2.91
2	2.95	-0.03	-0.04	2.92	2.91
3	2.99	-0.08	-0.08	2.91	2.91
4	2.94	-0.03	-0.03	2.91	2.91

- **S3. Protocols I to III applied to a test model**.

To substantiate the computational protocols used in the manuscript, we present the application of Protocols I to III to a reference compound of known structure. For this calculation we use the manganese complex *Aqua-(2-(((3-(methyl((pyridin-2-yl)methyl)amino)propyl)-((pyridin-2-yl)methyl) amino)methyl)phenolato)-manganese(ii) perchlorate* by Lassalle-Kaiser *et al.*,[4] which will be dubbed [**1**(OH_2)]$^+$, to follow the convention used by the authors. The high resolution CIF file of this compound (WAYNIV) is available as CCDC Number 691308.

Relevant Mn-scatterer distances are summarized in Table S17. Application of Protocols I to III, and their comparison with experimental data from Lassalle-Kaiser *et al.* is shown in Figure S11, and Table S18.

Table S17. Selected metal-scatterer lengths (Å) in [**1**(OH_2)]ClO_4 from X-ray diffraction data.

Shell	Atom pair	Length [Å]
1	Mn–O	2.0986
	Mn–O	2.1630
2	Mn–N	2.2447
	Mn–N	2.2783
	Mn–N	2.2923
	Mn–N	2.3269
3	Mn-C	3.0101
	Mn-C	3.0492
	Mn-C	3.0657
	Mn-C	3.0744
	Mn-C	3.0850
	Mn-C	3.1280
4	Mn-C	3.1629
	Mn-C	3.2144
	Mn-C	3.2208
	Mn-C	3.2224
	Mn-C	3.2254
5	Mn-C	3.4000
	Mn-C	3.5921

The progression from Protocol I to III shows a clear improvement in the quality of the fit. Changes in distances after application of Protocol III are very small, and well below the EXAFS resolution, except for the forth shell, in which an increase of 0.11 Å is obtained in the fitting. Inspection of Mn-C distances (Table S17) show that this shell contributes to the second peak, at around an apparent distance of 2.5 Å. The average distance of this shell extracted from X-ray

crystallographic data is 3.2 Å (Table S17). When increased to 3.3 Å (3.2 Å + 0.11 Å), it allows resolution of the third peak (marked with a green arrow in Figure S11), with concomitant reduction of the peak at 2.5 Å, which gives a better agreement with experiments. Also, this is consistent with the fitting based on shells in the source article, in which the best fit gives R=3.3 Å for this shell (Table S1 in Lassalle-Kaiser *et al.*).

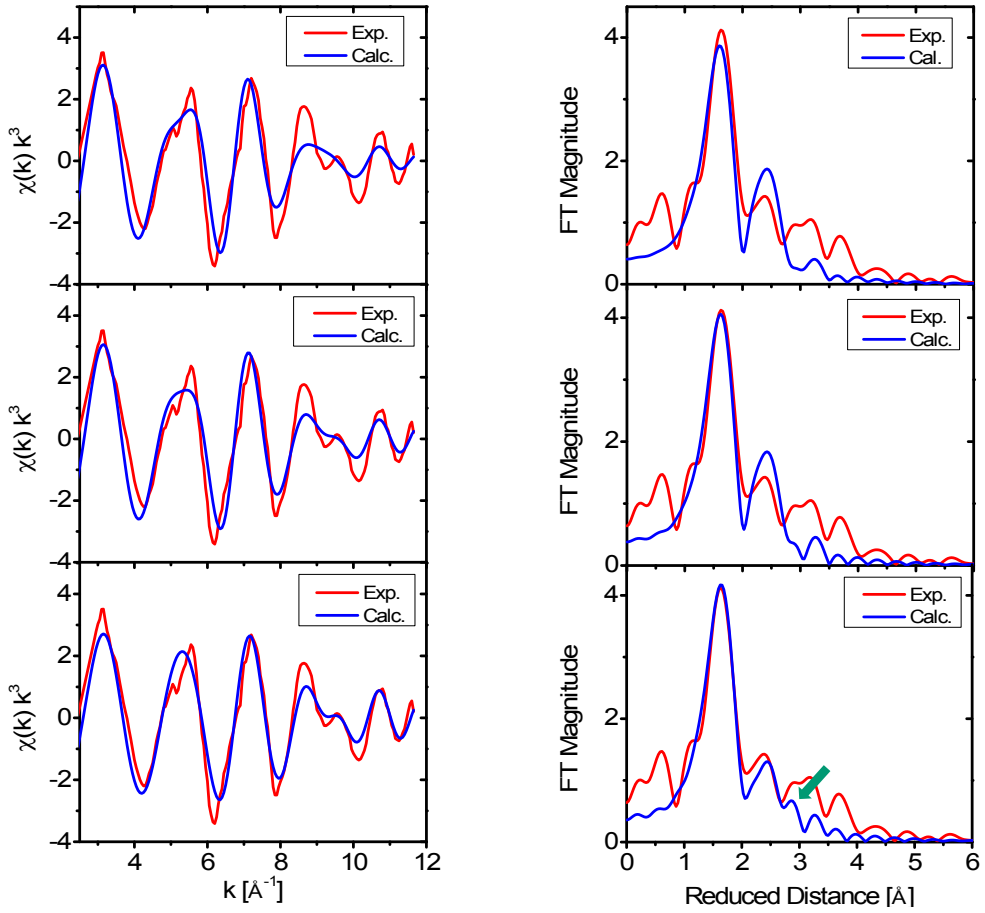

Figure S11. Mn (blue lines) *K*-edge EXAFS spectra simulations of [**1**(OH_2)]$^+$ using parameters computed with Protocol I (top), II (middle), and III (bottom). A green arrow shows the resolution of an extra peak after application of Protocol III. Experimental spectra from Lassalle-Kaiser *et al.* are shown with red lines. See Table S18 for details of the fittings.

Table S18. Fitting parameters of Mn and Fe *K*-edge EXAFS in Figure S11, obtained with Protocols I-III. For Protocol I, σ^2 (Å^2) taken from the best fit made in the original experimental study by Lassalle-Kaiser *et al*.

Protocol	S_0^2	**N**	**Shell**	σ^2 (Å^2)	ΔR (Å)[(a)]	ΔE_0 (eV)	*F*
I	**0.7**	**2.0**	Mn-O	**0.0020**	-	-5.60	0.586
		4.0	Mn-N	**0.0040**	-		
		6.0	Mn-C	**0.0050**	-		
		5.0	Mn-C	**0.0070**	-		
		2.0	Mn-C	**0.0020**	-		
II	**0.7**	**2.0**	Mn-O	0.0010	-	-5.55	0.480
		4.0	Mn-N	0.0028	-		
		6.0	Mn-C	0.0049	-		
		5.0	Mn-C	0.0106	-		
		2.0	Mn-C	0.0010	-		
III	**0.7**	**2.0**	Mn-O	**0.0010**	0.00	-5.41	0.406
		4.0	Mn-N	**0.0028**	-0.00		
		6.0	Mn-C	**0.0049**	0.02		
		5.0	Mn-C	**0.0106**	0.11		
		2.0	Mn-C	**0.0010**	-0.00		

(a) EXAFS resolution is ~0.15 Å. Bold numbers show the fixed parameters.

S4. Cartesian coordinates of models 1-4, optimized with the combined 6-31G basis set

Model **1**

71

C	5.305011	-2.047388	-2.159928
C	4.581665	-2.893273	-1.099822
C	3.933364	-2.009986	-0.024017
O	2.974098	-1.267816	-0.495510
O	4.380656	-2.001988	1.126062
C	2.619430	1.470538	-4.166767
C	1.302444	1.958781	-3.550082
C	0.839497	1.153775	-2.332564
O	1.734875	0.818939	-1.494545

O	-0.397706	0.897155	-2.248065
C	5.010083	1.079942	0.481624
C	3.900012	1.589163	1.345607
N	2.579536	1.144871	1.304899
C	3.996594	2.543130	2.326890
C	1.916271	1.812443	2.240016
N	2.736911	2.666721	2.881312
C	-4.432443	-3.635317	-0.202844
C	-3.268173	-3.122355	-1.060738
C	-3.550911	-1.761814	-1.715665
O	-4.687937	-1.495236	-2.118053
O	-2.528181	-0.961017	-1.868277
C	-2.952400	-0.262804	3.952633
C	-3.292752	-1.459439	3.053226
C	-2.258098	-1.529288	1.932778
O	-1.248994	-2.236971	2.089236
O	-2.515339	-0.771776	0.917988
C	-5.055441	1.424589	-0.431384
C	-3.866333	2.336797	-0.442116
N	-2.538253	1.911844	-0.463066
C	-3.880308	3.708966	-0.408131
C	-1.790642	3.004718	-0.435616
N	-2.559052	4.114686	-0.403590
H	4.599296	-1.389011	-2.675605
H	6.081140	-1.423194	-1.700748
H	5.789655	-2.685641	-2.908544
H	5.284356	-3.573957	-0.608352
H	3.801934	-3.495547	-1.582368
H	2.905680	2.104587	-5.013504
H	3.424729	1.492012	-3.427588
H	2.525481	0.441605	-4.532298
H	1.417462	3.001055	-3.218119
H	0.493422	1.948735	-4.286522
H	5.280925	0.061809	0.772440

H	4.711427	1.057720	-0.570636
H	5.885637	1.729051	0.586343
H	4.837772	3.125263	2.669814
H	0.864638	1.690794	2.441801
H	2.471119	3.278532	3.639557
H	-5.351946	-3.687163	-0.793620
H	-4.214642	-4.633160	0.195431
H	-4.615999	-2.964217	0.642931
H	-3.075351	-3.832259	-1.879476
H	-2.348262	-3.061505	-0.475674
H	-3.655820	-0.181264	4.789997
H	-2.991119	0.671916	3.382705
H	-1.943166	-0.367693	4.366488
H	-4.298199	-1.340789	2.635291
H	-3.256628	-2.388762	3.630815
H	-5.976611	2.014513	-0.473184
H	-5.038320	0.722278	-1.271592
H	-5.071953	0.818425	0.482017
H	-4.697727	4.413124	-0.385908
H	-0.712465	3.014283	-0.427830
H	-2.223031	5.066901	-0.386099
O	-0.023700	0.658576	0.584097
O	1.333304	-1.335950	1.697855
H	0.389836	-1.629261	1.762682
O	0.216974	-1.424097	-0.721142
H	0.561770	-1.561083	-1.610099
Mn	1.434775	-0.292867	0.246275
Fe	-1.366523	-0.033313	-0.561137

Model **2**

72

C	5.305006	-2.047389	-2.159922
C	4.393474	-2.909904	-1.277434

C	3.496878	-2.170824	-0.283834
O	3.010861	-1.034451	-0.666638
O	3.244919	-2.714073	0.814482
C	2.619429	1.470539	-4.166765
C	1.219798	1.919968	-3.731016
C	0.731745	1.246734	-2.457016
O	1.651553	0.994287	-1.590527
O	-0.486418	0.985143	-2.324042
C	5.010085	1.079944	0.481619
C	3.897876	1.763255	1.202654
N	2.547349	1.441975	1.076897
C	4.007552	2.787923	2.106281
C	1.877399	2.253151	1.892341
N	2.726078	3.078545	2.528290
C	-4.432443	-3.635316	-0.202845
C	-3.274285	-3.103361	-1.059117
C	-3.577098	-1.741319	-1.690550
O	-4.704048	-1.468353	-2.093853
O	-2.556103	-0.913604	-1.823347
C	-2.952398	-0.262806	3.952629
C	-3.076384	-1.516861	3.074662
C	-2.010233	-1.445302	1.994070
O	-0.906267	-1.983153	2.202824
O	-2.342651	-0.761695	0.949600
C	-5.055439	1.424589	-0.431383
C	-3.885463	2.356967	-0.420908
N	-2.548474	1.956276	-0.438682
C	-3.920576	3.726791	-0.366381
C	-1.817491	3.064104	-0.390267
N	-2.607246	4.154304	-0.347599
H	4.722209	-1.330303	-2.745299
H	6.026316	-1.484390	-1.556921
H	5.868200	-2.682150	-2.852107
H	4.973884	-3.640080	-0.705238

H	3.712748	-3.491299	-1.916673
H	2.900205	1.970835	-5.099700
H	3.366267	1.711510	-3.406494
H	2.650104	0.389619	-4.340893
H	1.213443	3.003363	-3.544475
H	0.473865	1.731647	-4.508484
H	5.143661	0.052456	0.836054
H	4.822611	1.029584	-0.594311
H	5.944647	1.622721	0.651071
H	4.871862	3.318077	2.474420
H	0.808004	2.243957	2.020408
H	2.461913	3.780909	3.205437
H	-5.354866	-3.678029	-0.788746
H	-4.207433	-4.640350	0.170641
H	-4.611243	-2.983814	0.659031
H	-3.080875	-3.797666	-1.890022
H	-2.349197	-3.042173	-0.481307
H	-3.689444	-0.279279	4.763115
H	-3.117856	0.644129	3.361200
H	-1.955271	-0.202870	4.402620
H	-4.070905	-1.561537	2.620308
H	-2.916680	-2.417996	3.673886
H	-5.986465	1.998642	-0.455381
H	-5.031176	0.746692	-1.290785
H	-5.061646	0.795710	0.467095
H	-4.750181	4.415834	-0.338042
H	-0.740142	3.095501	-0.376533
H	-2.289945	5.113121	-0.315704
O	-0.008211	0.819973	0.496587
O	1.464551	-1.067815	1.675192
H	0.530249	-1.450086	1.794690
O	0.260703	-1.250525	-0.755720
H	0.586693	-1.554517	-1.620177
H	2.121237	-1.825091	1.472124

Mn	1.437496	0.003787	0.043452
Fe	-1.439252	0.059278	-0.601872

Model **3**

71

C	-5.377505	-2.569091	1.198060
C	-4.634636	-3.049335	-0.060384
C	-3.934137	-1.877434	-0.762282
O	-2.923732	-1.411646	-0.092586
O	-4.389434	-1.425202	-1.819635
C	-2.731644	-0.053117	4.405026
C	-1.218729	-0.053573	4.160565
C	-0.818257	-0.047069	2.683434
O	-1.707290	0.020161	1.814882
O	0.455135	-0.125250	2.470646
C	-5.056233	1.314676	-0.089485
C	-3.916938	2.205302	-0.476365
N	-2.595657	1.778083	-0.569254
C	-3.966022	3.536441	-0.806711
C	-1.879937	2.827076	-0.947905
N	-2.668691	3.912381	-1.102744
C	4.391289	-3.337720	-1.070820
C	3.244306	-3.072930	-0.083989
C	3.609082	-2.084628	1.035291
O	4.765186	-2.064312	1.473903
O	2.648431	-1.352857	1.538192
C	2.958130	1.339395	-3.698127
C	3.523337	0.127225	-2.947658
C	2.416000	-0.424093	-2.054646
O	1.517923	-1.102530	-2.562599
O	2.524977	-0.051050	-0.813627
C	4.994494	1.274524	1.028251
C	3.797889	2.009896	1.553778

N	2.465988	1.598088	1.455420
C	3.818736	3.226058	2.189727
C	1.729169	2.550053	2.009583
N	2.506011	3.550822	2.470047
H	-4.678237	-2.115863	1.908171
H	-6.135080	-1.818969	0.941006
H	-5.886571	-3.401633	1.698390
H	-5.335711	-3.511769	-0.762846
H	-3.885018	-3.798388	0.222012
H	-2.940820	-0.067833	5.480889
H	-3.201743	0.836331	3.974791
H	-3.203956	-0.929287	3.950416
H	-0.743777	0.816220	4.634132
H	-0.746449	-0.930095	4.621607
H	-5.168810	0.498351	-0.809537
H	-4.883920	0.862388	0.893623
H	-5.986109	1.891105	-0.048813
H	-4.791722	4.229136	-0.859820
H	-0.812040	2.813722	-1.102960
H	-2.362158	4.827595	-1.400037
H	5.287323	-3.670824	-0.538950
H	4.107984	-4.105299	-1.800125
H	4.652924	-2.428139	-1.623394
H	2.973055	-4.015322	0.416947
H	2.346717	-2.731845	-0.602778
H	3.704171	1.768069	-4.377870
H	2.650137	2.123179	-2.996743
H	2.083327	1.048308	-4.288168
H	4.396925	0.411348	-2.353469
H	3.818833	-0.650407	-3.660122
H	5.904105	1.817151	1.304676
H	5.048886	0.253818	1.421347
H	4.954187	1.194791	-0.063470
H	4.641276	3.871847	2.455255

H	0.653889	2.539901	2.071961
H	2.178626	4.383180	2.938939
O	0.189562	0.979795	0.012864
O	-1.149815	-0.371872	-2.210426
H	-0.218207	-0.654485	-2.349871
O	0.201090	-1.482333	0.130783
H	0.105435	-2.110591	0.855391
Mn	1.345505	-0.096428	0.702464
Fe	-1.426722	-0.129861	-0.408371

Model **4**

72

C	5.355884	-2.022799	-2.040686
C	4.486282	-3.022877	-1.266715
C	3.447212	-2.430941	-0.310059
O	2.972566	-1.266505	-0.612476
O	3.084689	-3.107345	0.676118
C	2.661263	1.445797	-4.119916
C	1.143622	1.479188	-3.883886
C	0.732572	0.969530	-2.508294
O	1.652526	0.791116	-1.666422
O	-0.514137	0.750837	-2.308759
C	4.993964	1.128826	0.563392
C	3.878516	1.723574	1.361171
N	2.544715	1.342110	1.235173
C	3.955119	2.702877	2.317457
C	1.849373	2.076547	2.098151
N	2.666150	2.909420	2.770004
C	-4.389864	-3.691156	-0.194941
C	-3.227151	-3.076973	-0.994408
C	-3.577778	-1.741845	-1.663496
O	-4.712083	-1.544426	-2.091182
O	-2.603030	-0.864218	-1.845761

C	-2.999635	-0.260064	3.943561
C	-3.349981	-1.294025	2.864150
C	-2.218923	-1.319788	1.846755
O	-1.188274	-1.949767	2.103667
O	-2.466502	-0.598037	0.788854
C	-5.061625	1.359329	-0.485363
C	-3.851030	2.240659	-0.581356
N	-2.509685	1.833640	-0.609666
C	-3.870935	3.611310	-0.625185
C	-1.774039	2.939481	-0.659145
N	-2.557841	4.031794	-0.674638
H	4.737655	-1.341844	-2.631994
H	5.966450	-1.417554	-1.361514
H	6.032182	-2.555305	-2.718161
H	5.102256	-3.717917	-0.686874
H	3.920327	-3.642776	-1.977582
H	2.887669	1.802938	-5.130370
H	3.187750	2.081354	-3.402998
H	3.052663	0.429319	-4.018499
H	0.751384	2.500174	-3.986806
H	0.607854	0.881131	-4.629908
H	5.139677	0.071683	0.809159
H	4.787851	1.184719	-0.510101
H	5.926614	1.661972	0.769046
H	4.796273	3.256685	2.704101
H	0.781241	2.017620	2.237233
H	2.380552	3.563706	3.485554
H	-5.275054	-3.800683	-0.827424
H	-4.110406	-4.676394	0.193607
H	-4.662273	-3.054649	0.654169
H	-2.949005	-3.759469	-1.811850
H	-2.333985	-2.964894	-0.376309
H	-3.775114	-0.229263	4.716714
H	-2.912712	0.743560	3.512414

H	-2.048456	-0.512706	4.423004
H	-4.296420	-1.040680	2.378711
H	-3.434677	-2.289930	3.310374
H	-5.962409	1.977707	-0.533828
H	-5.089026	0.616672	-1.288730
H	-5.069633	0.806662	0.461125
H	-4.697875	4.304051	-0.621070
H	-0.697347	2.967160	-0.669304
H	-2.234266	4.988035	-0.718744
O	-0.185306	0.746330	0.427611
O	1.386346	-1.420810	1.751658
H	0.433046	-1.709536	1.827093
H	1.959159	-2.202572	1.461234
O	-0.134813	-1.400058	-0.706894
H	-0.138111	-1.787336	-1.590467
Mn	-1.382058	0.018556	-0.642881
Fe	1.444939	-0.161001	0.128504

References

1. E. A. Stern, D. E. Sayers and F. W. Lytle, *Phys. Rev. B*, 1975, **11**, 4836-4846.
2. A. V. Poiarkova and J. J. Rehr, *Phys. Rev. B*, 1999, **59**, 948-957.
3. J. J. Rehr and R. C. Albers, *Rev. Mod. Phys.*, 2000, **72**, 621-654.
4. B. Lassalle-Kaiser, C. Hureau, D. A. Pantazis, Y. Pushkar, R. Guillot, V. K. Yachandra, J. Yano, F. Neese and E. Anxolabehere-Mallart, *Energy & Environmental Science*, 2010, **3**, 924-938.